Thesis report

R.N.J. Boelhouwer

May 2023

Assessing the performance of the sonAIR aircraft noise model in predicting noise levels at Schiphol Airport

by

R.N.J. Boelhouwer

to obtain the degree of Master of Science in Aerospace Engineering
at the Delft University of Technology,
to be defended publicly on 9 May 2023 at 13:00.

Student number:	4346858	
Project duration:	September 5, 2022 – May 9, 2023	
Thesis committee:	Prof. dr. D. G. Simons,	Chairman
	Prof. dr. ir. M. Snellen,	Supervisor
	Dr. A. Bombelli,	Examiner
	ir. R. C. van der Grift,	Additional

An electronic version of this thesis is available at http://repository.tudelft.nl/.

Preface

Since the start of my bachelor in September 2014, I have learned a great deal on many aspects of aerospace engineering. If you would have asked me then, I do not think I would have shown a great interest in aircraft noise, and I definitely would not have expected to graduate on the topic.

However, during the first course on aircraft noise, I was starting to get interested. It is a highly relevant topic, which is often in the news. Also, noise is a natural, tangible topic which is all around us. These things eventually motivated me to do a thesis on aircraft noise.

The road towards graduation has not always been easy and without setbacks along the way. I am proud of what I have achieved, and I could not have done this on my own.

First of all, I would like to thank my supervisor Mirjam Snellen for her help during the thesis. At the start of the thesis, you really helped me regain my confidence and trust towards myself and the TU Delft. You showed great confidence in my capabilities, which I needed at the time. I would also like to thank Dick Simons for his critical view and feedback.

A special thanks goes out to my daily supervisor, but most of all friend, Rebekka. Since starting our bachelor together, we have been close friends inside and outside our studies. To end my studies working together on a project with you is somewhat symbolic, and very typical for the whole master's programme. I am grateful for your help, but even more so for you as a friend.

For the installation and explanation of sonAIR I would like to thank Christoph Zellmann from n-Sphere AG in Zürich. Without your help it would not have been possible to carry out this research. Our good contact ensured a smooth implementation and understanding of sonAIR. Your extensive knowledge on the model also helped us a lot. I would also like to thank Empa in Switzerland, for providing the noise emission models. Especially Beat Schäffer, who has helped a lot with his feedback and flexibility regarding data requests. Next, I would like to thank KLM and KDC for providing FDR data.

I would like to thank my parents and my brother. Your support has never been in doubt, for which I am ever grateful. I would like to thank my friends for their noble support, and distraction when needed. It is a cliché, but I can definitely say that I have made friends for life during my time as a student in Delft.

Finally, I would like to thank Noëlle for her love and support during the thesis, which was very much needed. I hope to return the favour next year.

Robbert N.J. Boelhouwer
Delft, April 2023

Cover image credit: DALL-E 2

Contents

I

Paper

Assessing the performance of the sonAIR aircraft noise model in predicting noise levels at Schiphol Airport

Robbert N.J. Boelhouwer
Delft University of Technology, Delft, the Netherlands

Aircraft noise is a significant problem for communities surrounding airports. Accurate prediction models are needed to estimate noise levels from aircraft operations. In this research, the accuracy of the sonAIR aircraft noise model is evaluated in predicting noise levels around Schiphol airport by comparison to measurement data from NOMOS and the current best-practice modelling approach Doc29. Results show a significant but consistent underestimation of noise levels by sonAIR, mainly due to a generalisation of emission models. The standard deviation of differences between model results and measurements is lower for sonAIR than for Doc29 by up to 1 dB. Differences between measurement and model results were found in the relation between N1 and noise levels, maximum noise levels and frequency spectra. These results demonstrate that sonAIR provides more reliable predictions of noise levels on the single flight event level than Doc29. Additionally, this study shows agreement with results from a previous validation study in Zürich, thereby confirming the applicability of sonAIR to another airport. This research contributes to better aircraft noise predictions, which will have implications ultimately leading to a better quality of life for communities affected by aircraft noise.

Nomenclature

L_{AE}	=	Sound exposure level
$L_{A,max}$	=	Maximum A-weighted noise level
μ	=	Mean value
σ	=	Standard deviation
B737NG	=	Boeing 737 Next Generation series
B738	=	Boeing 737-800
FDR	=	Flight Data Recorder
NMT	=	Noise Monitoring Tower
NOMOS	=	NOise MOnitoring System
NPD	=	Noise-Power-Distance
PBL	=	Pressure Band Level
PCC	=	Pearson Correlation Coefficient

I. Introduction

Aircraft noise is a significant concern for communities located near airports, as it can affect the quality of life of residents and contribute to hearing loss and other health problems [1]. In order to mitigate the impact of aircraft noise on communities, it is important to accurately predict and measure the level of noise that will be generated by aircraft operations. There are various models that have been developed for this purpose, each with their own strengths and limitations. In general, two types of noise models are differentiated: non-empirical and empirical models [2]. Non-empirical models, or theoretical models, are formed on a mathematical basis, describing the noise emission and propagation. Empirical noise prediction models are based on noise measurements.

In Europe, the European Civil Aviation Conference (ECAC) Doc29 modelling approach is the current best-practice modelling approach [3]. This is an empirical method which makes use of Noise-Power-Distance (NPD) tables, which provide a noise value for an aircraft at a certain distance given its thrust setting.

Alternatively, the sonAIR aircraft noise model was created by the Swiss Federal Laboratories for Materials Science and Technology (Empa). Their goal was to fill the gap between best practice approaches for long-term averages on one side, and highly detailed, computationally expensive models on the other side. The model was based on backpropagation of flyover measurements from an extensive measurement campaign around Zürich airport. It is able to simulate single noise events with a high level of detail, but also perform noise mapping for airports [4]. However, no independent validation study for sonAIR has been conducted, and it has not been applied to airports outside Switzerland yet.

The aim of this study is to apply and validate the sonAIR noise model on noise data from Schiphol airport, by comparing its performance to measurements (NOMOS) and current best-practice modelling approach (Doc29) around the Netherlands' largest airport. Each of these methods are explained in section II. The input data is elaborated upon in section III. Validation results are given in section IV and are discussed in section V. Finally, conclusions are drawn and an outlook is given in section VI.

II. Methods

A. NOMOS measurements

The NOise MOnitoring System (NOMOS) entails 41 noise monitoring towers (NMTs) around Schiphol airport. A NMT consists of a six to ten meter high tower with a calibrated microphone on top of it. This is an ISO class 1 microphone, which constantly measures all sounds in its environment [5] [6]. The measurement uncertainty of a station is 0.7 to 0.9 dBA [6]. An overview of the NMT locations can be seen in Figure 1.

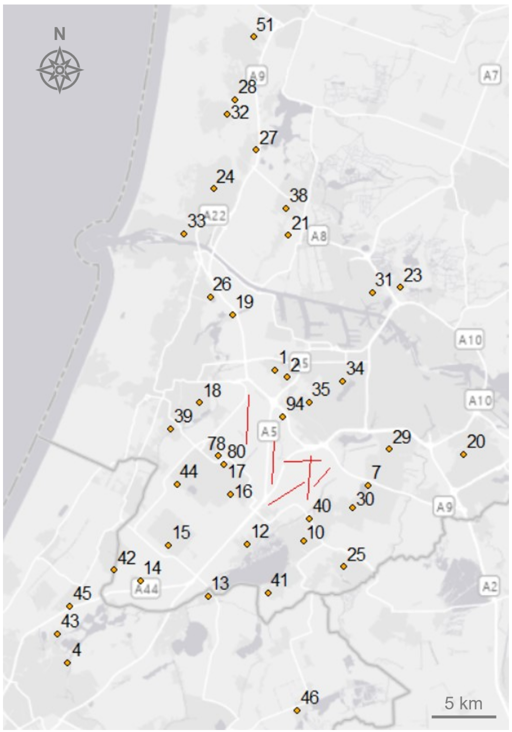

Fig. 1 NOMOS NMT locations

It is important to be able to distinguish an aircraft-related noise event from other sounds. Therefore, noise events are defined by fixed thresholds. Each NMT has its own threshold in dBA, depending on the background noise. The noise event starts when the measured sound passes the threshold. Further requirements on the noise events are as follows [7]:

- The duration of the event should be at least 10 seconds and at most 120 seconds;
- The maximum noise level ($L_{A,max}$) of the noise event must be at least 12 dBA higher than the background noise level;
- This $L_{A,max}$ must be the local maximum for 30 seconds before and after the event;
- The sound exposure level (L_{AE}) of the event must be between 7 and 13 dBA above the $L_{A,max}$.

The NOMOS information is processed and stored in the Airport Noise and Operations Management System (ANOMS) application managed by Envirosuite [8]. A noise event is automatically stored if it meets the requirements, and, if possible, it is linked to a flight using radar data.

B. sonAIR aircraft noise model

The sonAIR aircraft noise model consists of two parts: an emission model and a propagation model. Each model is formulated for 24 1/3-octave bands, with a frequency range from 25 Hz to 5 kHz. The emission model is specific per aircraft type.

The emission models were established after an extensive measurement campaign at Zürich airport. This microphone data, together with Flight Data Recorder (FDR) data, flight profiles and meteorological data, provided the input data for the backpropagation process. Based on these inputs, linear regression models were established for each 1/3-octave band. The emission models are further split into an airframe and engine noise model. By doing so, both sound sources can be modelled separately. Most aircraft types use a reduced model; for some aircraft types, an advanced emission model is available. These models use three additional aircraft configuration parameters as input.

This method requires a lot of data to be able to create a reliable model, including measurements at different locations for many flight events. In addition, each aircraft (sub)type needs its own model. As a consequence, a limited number of aircraft types have been added to the sonAIR model.

Two modes exist to calculate sound propagation: direct calculations and sonX calculations. Direct calculations only account for the direct path between source and receiver and the attenuation in between. The propagation model sonX was originally developed for train and shooting noise, but modified to be able to be used for aircraft noise [9]. It is formulated for point sources and calculates sound both directly and reflected. It accounts for atmospheric absorption, ground effect, foliage attenuation, and the influence of vertical gradients of wind, temperature, and relative humidity [9] [10].

1. Model inputs

Like any noise prediction model, sonAIR uses several input parameters. An elaborate explanation of the use of each parameter is given in Zellmann et al. [9], a brief description is presented in this section. An overview of all input parameters can be seen in Figure 2.

N1 is the engine rotational speed in %. This parameter was chosen to represent the engine, because it can be determined using spectrograms when FDR data is not available, unlike e.g. the thrust setting [10]. It is correlated to the jet velocity, which is a main contributor to engine noise. To determine the relation between N1 and the sound pressure level (SPL), an engine run-up test was performed on an Airbus A330-300 with the TRENT772B engine. The SPL was measured at a distance of 170 meters from the aircraft, at four locations: 15°, 50°, 90° and 120° respectively, with 0° corresponding to the nose of the aircraft. The results provided a second order polynomial for each 1/3-octave band.

The aircraft **Mach number** is chosen to account for speed-dependent sound sources. It influences both the engine noise and airframe noise level. For engine noise, a linear relation is used. i.e. $L_{em,eng} \propto Ma$. A logarithmic relation is derived for airframe noise: $L_{em,afm} \propto \log_{10}(Ma)$, which represents the physics of airframe noise better than a linear relation.

Only the **air density** ρ is chosen as atmospheric parameter. The air pressure p and temperature T were omitted because of the close relation between the three, which might lead to multicollinearity.

The directivity of aircraft sound emission can be described using spherical coordinates. The engine noise differs along the **polar angle** θ and the **azimuth angle** ϕ.

A binary variable is used to indicate the procedure of the aircraft. The **procedure input** $Proc$ is either departure or landing.

For advanced emission models, the aircraft configuration is described in three variables: **landing gear** (LG, 0: retracted, 1: deployed), **flap handle position** ($Flaps$, 0 to 4, depending on deflection) and **speed brakes** (SB, 0: not deployed, 1: deployed).

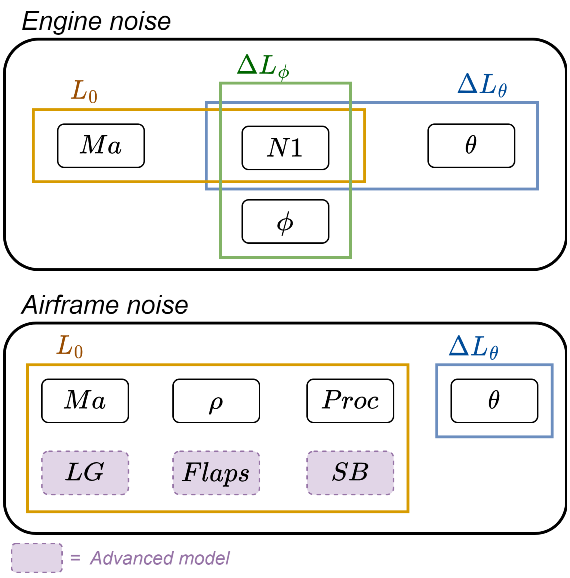

Fig. 2 sonAIR input parameters

2. Regression model

Before regression models are created, the dataset is split in two subsets. The first subset contains data for idle engines ($N1 \leq 40\%$) and the second subset all data for engines on-load ($N1 > 40\%$). The former includes only approaches, the latter both approaches and departures. This separation of the dataset allows for the creation of two different regression models: one for airframe noise and one for engine noise.

The airframe noise model consists of a source term (L_0) and a radiation term (ΔL_θ):

$$L_{em,afm}(f) = L_{0,afm}(lMa, l\rho, Flaps, LG, SB, Proc) + \Delta L_{\theta,afm}(\theta), \quad (1)$$

with $lMa = \log_{10}(Ma)$ and $l\rho = \log_{10}(\rho/\rho_0)$. This transformation of input variables is done to ensure a linear relation with L_{em}.

The engine noise model consists of a source term (L_0) and two radiation terms (ΔL_θ and ΔL_ϕ):

$$L_{em,eng}(f) = L_{0,eng}(Ma, N1) + \Delta L_{\theta,eng}(\theta, N1) + \Delta L_{\phi,eng}(\phi, N1). \quad (2)$$

For the reduced models, the aircraft configuration variables can no longer be used. This changes the airframe model, the engine model remains the same.

3. Model verification

In Zellmann et al. [9], the performance of the model is evaluated using the coefficient of determination R^2 and the root mean square error $\hat{\sigma}_E$. Two aircraft are selected for a detailed evaluation, the Airbus A320 and the Embraer E170. In general, a good correlation is found for the regression models, with R^2_{total} between 0.7 and 0.8 approximately. The engine model performs best, with R^2_{eng} above 0.8 for almost all frequency bands. The airframe model performs worse, with R^2_{afm} values between 0.2 and 0.6; however, it peaks in frequency ranges in which airframe noise is significant. The root mean square error $\hat{\sigma}_E$ shows similar behaviour for both aircraft, with values between 4.5 dB (low frequencies) to 3 dB (mid to high frequencies).

These results lead to the belief that sonAIR is a suitable model for predicting and assessing aircraft noise. The relevance of the model will increase if it will be tested and validated for more aircraft types and airports.

4. Model validation

In a validation study by Jäger et al. [4], over 20,000 noise events around Zürich and Geneva airport were simulated and compared to measurements. The reduced and advanced models were evaluated separately. Overall, the advanced models perform well, with almost all aircraft types having a mean difference and standard deviation below values of ±1 dB and 2 dB respectively. The reduced models show an average increase in standard deviation of about 0.7 dB when compared to the advanced models. This difference may be due to the models using less information (no FDR data), both during creation and simulation.

The land cover data was identified as the most influential input parameter. Especially in urban areas, a coarse grid may not differentiate between e.g. a park and (highly reflective) buildings, which can lead to deviations.

An interesting discovery is the seasonal effect of the model accuracy. It is found that the model is quite accurate during the summer months, but underestimates the noise levels in winter. Jäger et al. suspect that this may be (partially) due to the fact that all measurements used to set up the model were conducted during spring and summer.

In a comparison study by Meister et al. [11], sonAIR is compared to two other aircraft noise prediction models, FLULA2 and AEDT. It is concluded that sonAIR outperforms these two models when FDR data is available. For simulations without FDR data, all three models produced similar results. Additionally, sonAIR performs better for detailed single flight simulations.

In another validation performed by Jäger et al. [12], sonAIR was compared to measurements around Schiphol airport in collaboration with Delft University of Technology. A total of 74 overflights were measured, using a microphone array consisting of 32 microphones. The results show a mean difference of -0.4 dB, with a standard deviation of 1.1 dB. These results are a first step in demonstrating the applicability of sonAIR to different airports.

C. Doc29 noise model

The Doc29 noise model is the current best-practice method and was developed by ECAC. This approach is the result of the need for a harmonised European approach to noise modelling. The method is described in Volume 1 [13], implementation and verification are presented in Volumes 2 [14] and 3 [15], respectively. It is a modelling technique rather than a ready-to-use model. Doc29 makes use of NPD tables. These tables provide information on the relationship between the noise produced by an aircraft, its power setting and the distance to the observer.

One of the advantages of using NPD tables is that they provide a consistent and standardised method which allows for fast evaluation of the noise impact of aircraft operations. On the other hand, the standardisation is also one of the disadvantages, as it may lead to more inaccuracies.

III. Data

In this research, two main sources of data are consulted. First, KLM Royal Dutch Airlines (KLM) provided FDR data for a selection of flights. This is information from on-board the aircraft, which updates every second. Second, the ANOMS software provides radar track data and measurement data. The radar track data is updated every four seconds. Measurement data is available for both flights with FDR tracks and flights with radar tracks.

A. Aircraft selection

To limit the scope of the research, the focus is put on one aircraft type. A table containing all considered aircraft can be found in Appendix A. The aircraft type that was identified as most interesting and relevant is the Boeing 737 Next Generation series (B737NG). This series entails the 737-700, 737-800 and 737-900. This aircraft is used frequently at Schiphol airport and by KLM, thus input data is widely available.

B. Position data

Data on the position of the aircraft can be described in latitude, longitude and altitude. This data is included in the FDR tracks and the radar tracks.

C. N1 determination

For the flights with FDR tracks, N1 data was included in the dataset and could thus directly be used as input. For the flights with radar tracks, N1 was determined following the method as described in Van der Grift [7]. In this method, N1 is estimated by finding the fan tone in the spectrogram of an acoustic measurement. A similar method has been used by Merino-Martínez et al. [3] and Schlüter et al. [16] [17].

D. Measurement data

The measurement data was retrieved from the ANOMS software. The main metrics used in this research are the sound exposure level (L_{AE}) and the maximum noise level ($L_{A,max}$), as both are commonly used to compare noise predictions. The measurement data also entails noise level time histories and frequency spectra for 1/3-octave bands from 16 Hz to 16 kHz.

E. Meteorological conditions

To check the validity of measurement data, meteorological conditions were obtained from the Royal Netherlands Meteorological Institute [18]. If in the hour of departure it is raining and/or the average wind speed is too high, the measurement is discarded. The upper limit for the wind speed was set at 8 m/s, since above that variability of noise levels increases [19].

Noise propagation calculations for sonAIR were carried out in *BASIC* mode, which does not account for meteorological conditions. To correct for this, the methodology as

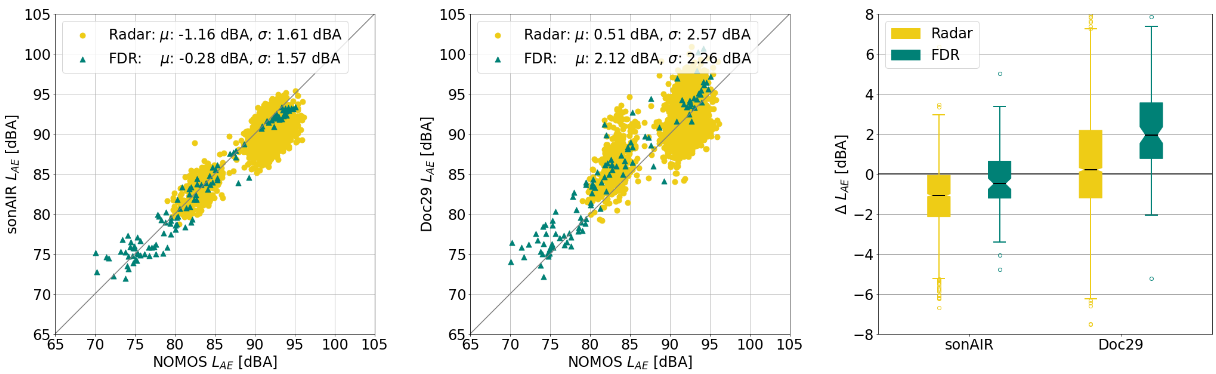

Fig. 3 Comparison of L_{AE} for B737NG departures (FDR: 112 events, radar: 2,761 events)

described in Appendix D of Doc29 Volume 2 [14] was used. This entails a correction for meteorological conditions that are different from ISA conditions (i.e. $T = 293.15K$, $p = 101,325Pa$ and $h_{rel} = 70\%$). This methodology makes use of the calculation corrections for atmospheric absorption as described in SAE-ARP-5534 [20].

F. Additional inputs

Two more inputs are required: a height map and landcover map, which are used to calculate sound reflections. The height map of the Netherlands is available via the Netherlands' Cadastre, Land Registry and Mapping Agency [21]. The landcover file was downloaded through Statistics Netherlands [22].

G. Sound propagation

In sonAIR, two modes exist to calculate sound propagation: direct calculations and sonX calculations. As the latter is deemed more accurate, this mode will be used for all calculations. A simulation will be performed using only direct calculations to determine the difference in model results between the two modes.

IV. Results

The simulated results give the noise levels for each desired source-receiver combination. An example noise level time history can be seen in Figure 4, where both models are compared to NOMOS data.

The 10 dBA down time line indicates the section of the curve which is used to calculate the L_{AE}. It can be seen that the sonAIR curve is approximately the same shape as the NOMOS curve. The NOMOS curve is less smooth than the model curves. Doc29 exhibits a wider curve, with longer rise and fall times of L_A.

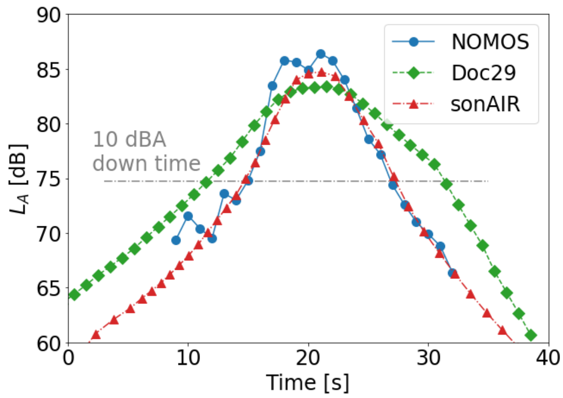

Fig. 4 Example noise level time history for B737NG departure

In this research, noise events are compared on an individual basis, mainly on their L_{AE} and $L_{A,max}$. Results are shown in the form of mean differences, which are calculated by subtracting the measurement result from the model result. The mean differences are expressed by mean values (μ) and the corresponding standard deviation (σ).

A. Model results

A distinction is made between flights with FDR data and flights with radar data. All flights were departing flights.

1. FDR data

For the flights where FDR data was available, a total of 112 events could be analysed, consisting of a mixture of 737-700 (15 events, or 13%), 737-800 (89, 80%) and 737-900 (8, 7%). The NOMOS measurement data for these events originates from eighteen different NMTs.

Figure 3 shows the comparison between L_{AE} results from sonAIR, NOMOS and Doc29 for both FDR and radar data. Looking at the FDR data, from the left plot, it can be seen that sonAIR shows fairly good agreement with mea-

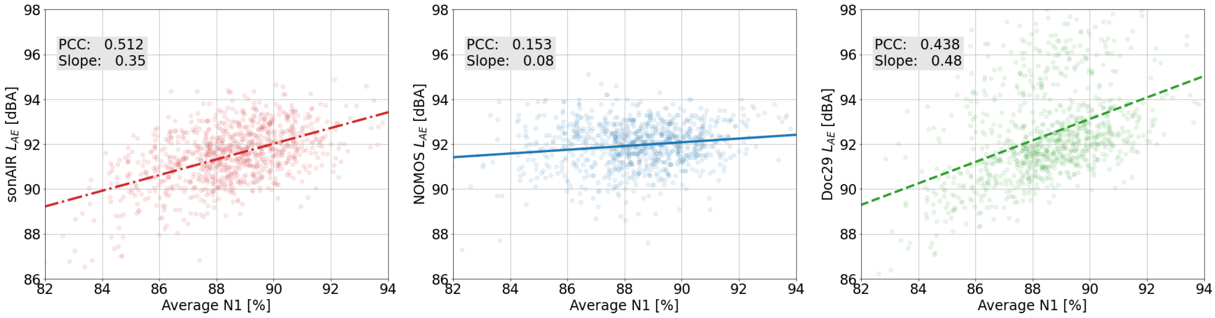

Fig. 5 Relation between N1 with L_{AE} for B738 data of NMT 94 (910 events)

surements, with $\Delta L_{AE} = -0.28 \pm 1.57$ dBA. Doc29 results, in the middle plot, deviate more and are more scattered, resulting in $\Delta L_{AE} = 2.12 \pm 2.26$ dBA. The boxplots display the same data. The notches represent the 95% confidence interval of the median. The boxes extend from the first quartile to the third quartile. The whiskers are drawn to the data point closest to and within the 1.5 interquartile range.

The plots comparing the $L_{A,max}$ can be found in Appendix B. The maximum levels show larger underestimations for sonAIR, i.e. $\Delta L_{A,max} = -2.29 \pm 1.93$ dBA. For Doc29 there is an overestimation, with $\Delta L_{A,max} = 1.87 \pm 2.08$ dBA.

2. Radar data

For the flights with radar data, total of 2,761 events were analysed, all of which are Boeing 737-800 (B738). The NOMOS measurement data was measured by NMTs 34, 40 and 94.

The L_{AE} results can be seen in Figure 3. The left plot shows for sonAIR $\Delta L_{AE} = -1.16 \pm 1.61$ dBA. The Doc29 results show a mean closer to the 1:1 line, but with a larger spread, i.e. $\Delta L_{AE} = 0.51 \pm 2.57$ dBA.

The maximum levels, again presented in Appendix B, show similar results. For sonAIR this is $\Delta L_{A,max} = -2.31 \pm 2.25$ dBA and for Doc29 $\Delta L_{A,max} = 0.60 \pm 2.76$ dBA.

B. Input parameters

The B738 radar data results were used to analyse the relation between input parameters and noise levels. The plots comparing the average N1 during the event to the L_{AE} for each event can be seen in Figure 5. The p-value for each plot is in the order of 10^{-6} or smaller.

What stands out is the positive correlation between N1 and L_{AE} in both models, which is not as apparent in the measurement data. Doc29 shows a steeper curve than sonAIR.

C. Frequency spectra

The L_{AE} results can be broken down into frequency components for each 1/3-octave band. An example frequency spectrum for a single noise event is given in Figure 6. This is the same event as depicted in Figure 4. The pressure band level (PBL) values are normalised such that the value at 1,000 Hz equals 70 dB. For Doc29, the ANP database [14] was consulted, which only contains data for 1/3-octave bands of 50 Hz and higher. It should be noted that this data is only used to carry out a correction for meteorological conditions, and not for SEL calculations or propagation calculations.

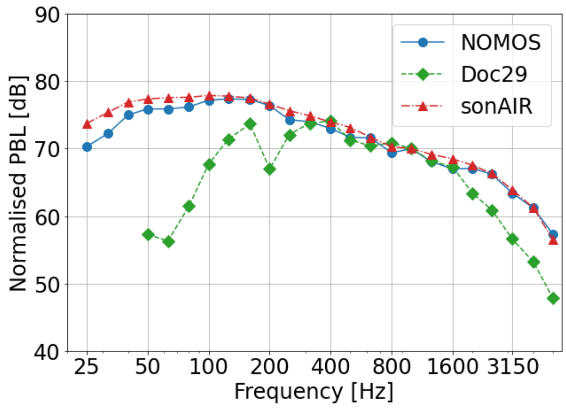

Fig. 6 Example noise spectrum for B737NG departure

To get an insight in the general performance of sonAIR in reproducing the noise spectrum, a comparison is performed for all noise events from the B737NG with FDR data. The NOMOS spectrum is subtracted from the sonAIR spectrum to get the ΔPBL. Subsequently, the ΔL_{AE} from the event is subtracted from each frequency band, to normalise the result to an overall difference of 0 dB.

Analysing all events resulted in large differences across the spectrum. The differences were particularly large at the lowest and highest frequencies. Upon further inspection it was found that a large influence on the presence or absence of these differences is the location of the NMT. A clear distinction was discovered between NMTs located directly

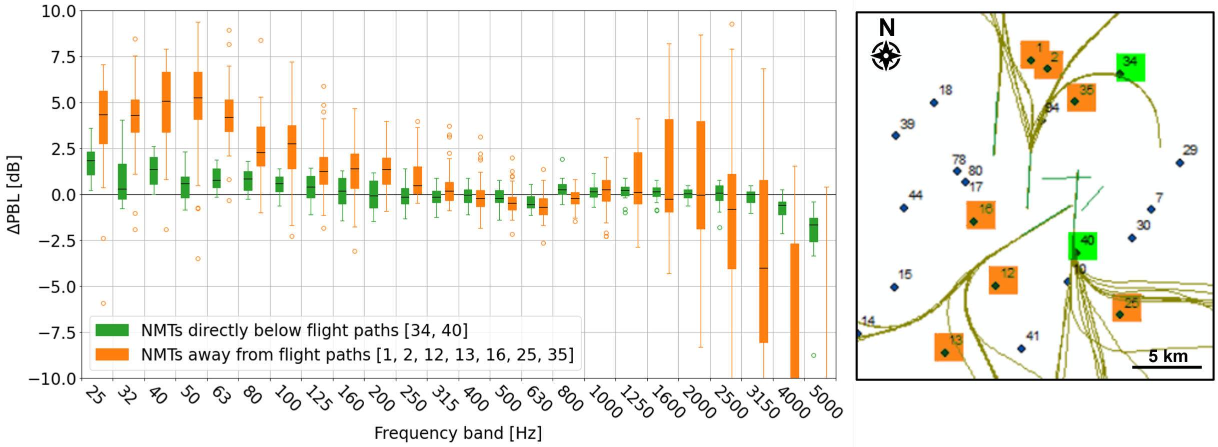

Fig. 7 Comparison of frequency spectra split by NMT location

below flight paths and NMTs further away from flight paths. The former show a good agreement overall. The latter show deviations in specific frequency ranges: firstly, the lowest frequencies (≤100 Hz) are generally overestimated. Secondly, the frequency bands between 1,250 - 2,500 Hz show a very large spread, with both large over- and underestimations. Thirdly, the highest frequencies (≥3,150 Hz) are underestimated, for the most part by a lot. The results can be seen in Figure 7, which includes a map showing the NMTs and flight paths.

D. Sound propagation

The B738 dataset with radar data was simulated with direct propagation calculations instead of sonX propagation calculations. This change in sound propagation mode yielded a decrease in mean values for L_{AE} and $L_{A,max}$ of 0.5 and 0.7 dB respectively, thus worsening the results.

V. Discussion

A. Model performance

1. sonAIR

The sonAIR model results show a fairly good agreement with measurement results, although there is an underestimation of L_{AE} and $L_{A,max}$. For L_{AE}, this underestimation is around -1.1 dB, which is in accordance with previous results by Jäger et al. [4]. The explanation given in their research is that the emission model is grouped for the B737 series, rather than having a model for each subtype. This leads to inaccuracies: with increase in size and mass also comes increasing underestimation of noise levels. Since the radar dataset contains only B738, underestimation of model results was to be expected.

Values for $L_{A,max}$ are underestimated more, with a mean value of -2.31 dB. A possible factor could be that this value is very sensitive, e.g. disturbances in the air might cause a peak in measurement values which is very difficult to model. However, the underestimation is too big and consistent to be solely attributed to variations in the air, thus other explanations are required.

Besides the mean values, differences between sonAIR results and measurements show relatively low values for standard deviation.This indicates that the model has a good precision and demonstrates the capability to accurately predict noise levels for single flight events.

Furthermore, there is better agreement for NMT 34 compared to NMTs 40 and 94. This NMT is located further from the runway than the other two, leading to lower noise levels. Looking at Figure 3, the lower left point cloud of the radar data shows results from NMT 34. NMTs 40 and 94 form the upper right point cloud. The data from NMT 34 is close to the 1:1 line, with $\Delta L_{AE} = 0.05 \pm 1.33$ dB.

2. Doc29

In general, Doc29 model results are similar to findings in previous research, with a mean difference between model results and measurements of less than 1 dB and standard deviations of around 2.5 dB.

However, it is notable that the FDR results deviate great from measurements, with a near consistent overestimation resulting in mean values of around +2 dB for both L_{AE} and $L_{A,max}$. A similar trend is visible for $L_{A,max}$. Radar results show a better overall agreement, but with a larger spread.

The standard deviations of Doc29 are relatively high, with values around 2.5 dB. Additionally, in contrast to sonAIR, the Doc29 results for NMT 34 are worse than NMTs 40 and 94.

3. Model comparison

Considering the mean values, Doc29 shows better performance than sonAIR in each case, with an exception for L_{AE} values with FDR data; however, the underestimation of mean values by sonAIR can be attributed to the grouping of emission models. Additionally, while sonAIR tends to underestimate noise levels, Doc29 generally overestimates them. This leads to large differences in mean results, which is particularly visible for the FDR dataset. It is remarkable that the mean $L_{A,max}$ value for sonAIR shows a 2.34 dB underestimation, whereas Doc29 overestimates by 1.82 dB.

The standard deviation of sonAIR is consistently lower, by up to 1 dB. Reducing the variability between measurements and model results is of importance, especially for modelling on single flight event level.

These results indicate that sonAIR provides more reliable noise predictions than Doc29 on the single flight event level.

B. Input data quality

The two main data sources for position data provide different quality of inputs. To determine the effect of this difference, the flights for which FDR data was available were also simulated using radar data. Boxplots showing the ΔL_{AE} results for both simulations are shown in Figure 8.

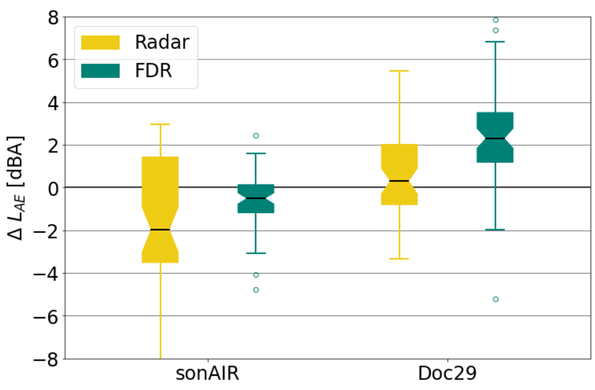

Fig. 8 Boxplots showing ΔL_{AE} for flights simulated with FDR data and radar data

It can be seen that sonAIR results clearly benefit from the higher quality of FDR inputs. This effect is not apparent in Doc29 results, for which the standard deviation is similar but a larger mean difference is found.

FDR data provide better results for sonAIR, but it is also scarcely available. Radar data on the other hand is more widely available. Since it is important to analyse sufficient events, radar data is a viable alternative when FDR data is not at hand.

C. N1 relation

In sonAIR, the relation between N1 and engine noise is modelled by a quadratic function, which assumes noise levels to increase with N1 for higher N1 values. A similar assumption is made in Doc29, albeit a linear increase.

However, limited increase in noise levels was found from measurements for the N1 range between 80% and 100%. A similar discovery is made by Van der Grift [7], who found that this 20% thrust increase leads to less than 1 dBA increase in measured maximum noise level, which is considerably less than the 4 dBA assumed by Doc29. These findings raise questions about the validity of the assumptions made by these models.

Looking at example plot of the larger range of N1 values (20% - 100%) in Figure 9 (adapted from Zellmann et al. [9]), it can be seen why a quadratic relation was assumed for sonAIR. Due to the lower N1 values, a quadratic curve seems the best fit. For the higher values, this will lead to a significant increase in predicted noise levels, which may not always be in line with measurements.

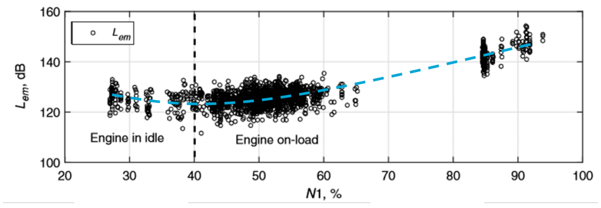

Fig. 9 N1 versus emitted noise for the A320 at 100 Hz. (Adapted from Zellmann et al. [9])

A solution could be to split the regression model in two different relations; one for N1 < 75% and one for N1 ≥ 75%. Since aircraft will either fly with a high N1 (departures) or low N1 (landings), there is a gap between roughly 70% and 80%, which is where the split can be made. Another option could be to assume a higher order relation, e.g. cubic, which will allow the regression to better fit to the data if a levelling of the measurement data occurs above 80%.

D. Frequency spectrum analysis

Analysing the frequency spectra revealed a clear distinction in the ability of sonAIR to accurately predict noise levels between NMTs below the flight path and NMTs further away. Where the former generally agrees well with measurement data, for the latter there are differences visible. Especially at the highest frequency bands, a large underestimation of the PBL is present.

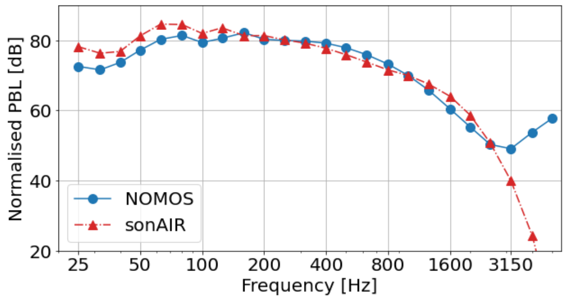

Fig. 10 Example frequency spectrum with peak at highest frequencies for NOMOS data

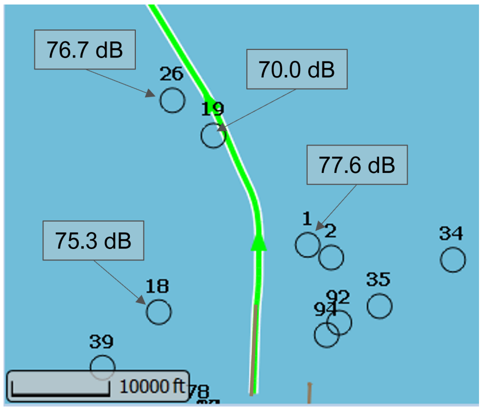

Fig. 11 Flight path with L_{AE} values of relevant NMTs (Adapted screenshot from ANOMS [8])

Looking at the PBL values of NOMOS and sonAIR themselves, rather than the differences, a few things can be noted. For sonAIR, the highest frequency bands always have the lowest PBL values, independent of the NMT location. On the contrary, NOMOS data will at times show an increase in PBL for the highest frequencies; this only happens at NMTs further away from the flight paths. An example can be seen in Figure 10.

It is unclear what the cause of this difference is. It may be due to propagation errors along the larger distances, differences in lateral directivity or contamination by background noise in the NOMOS data.

E. Sound propagation

The sound propagation calculation mode has a significant influence on the model results. The best results are achieved with sonX calculations. In Jäger et al. [4] it was determined that the resolution of the landcover file is also of great importance. Using sonX calculations in combination with a high resolution landcover file is thus recommended.

F. NMT 19 reliability

During this research, NMT 19 has been identified to at times give unreliable results or not produce results at all. In one particular case, NMT 19 gave values significantly lower than other NMTs despite being closer to the flight path, see Figure 11.

The simulated values by sonAIR and Doc29 are significantly higher, namely 81.4 and 81.8 dB respectively. These observations confirmed the belief that NMT 19 is inaccurate. Therefore, NMT 19 results were omitted.

VI. Conclusions and outlook

In this research, the sonAIR noise model was validated by comparing it to NOMOS measurements and the current best-practice modelling approach, Doc29, for the Boeing 737 Next Generation series at Schiphol airport. The results demonstrate that sonAIR provides more reliable predictions of noise levels on the single flight event level than Doc29. Additionally, this study shows agreement with results from a previous validation study in Zürich, thereby confirming the applicability of sonAIR to another airport.

For further research, more aircraft types can be analysed to examine the versatility of sonAIR. The relation between N1 and noise levels for high N1 values should be explored further. Additionally, the differences in maximum noise levels and frequency spectra require further attention.

Although sonAIR provides more reliable predictions than Doc29, improvements can still be made. Further measurements to update and refine the emission models are recommended, including separate models for aircraft subtypes, to improve the accuracy of noise predictions.

This research contributes to better aircraft noise prediction. Improvements in this field will have important implications for noise management around Schiphol airport and other airports worldwide, ultimately leading to a better quality of life for communities affected by aircraft noise.

Appendix

A. Aircraft selection

The table containing all considered aircraft is presented in Table 1.

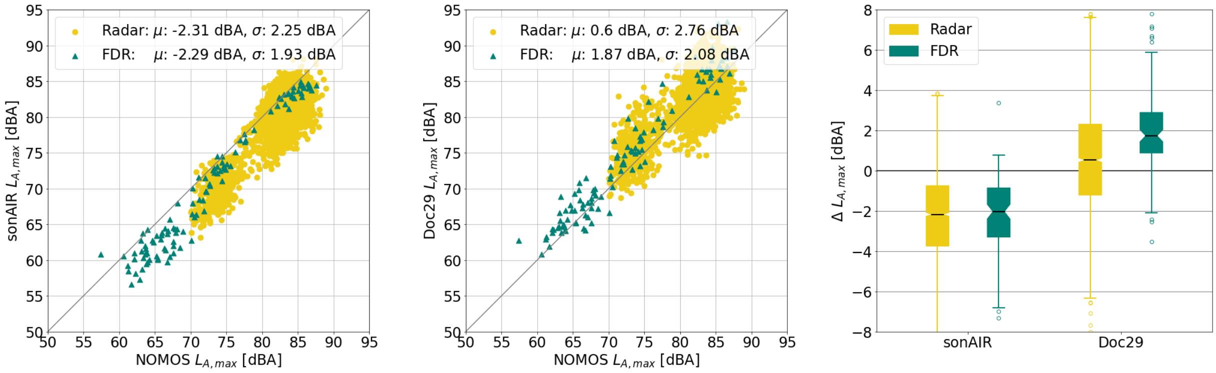

Fig. 12 $L_{A,max}$ **comparison for B737 series departures (FDR: 112 events, radar: 2,761 events)**

Table 1 Aircraft selection

Aircraft type	sonAIR	Schiphol	KLM
Airbus A320 family	Adv.*	Yes	No
Airbus A330 family	Adv.*	Yes	Yes†
Airbus A340 family	Adv.*	No	No
Airbus A380 family	Red.	Yes	No
BAe Avro RJ-100	Adv.	No	No
Boeing 737 Series	Red.	Yes	Yes
Boeing 747 Series	-	Yes	Yes
Boeing 767 Series	Red.	No	No
Boeing 777 Series	Adv.*	Yes	Yes
Boeing 787 Series	-	Yes	Yes
Bomb. CRJ-900	Red.	No	No
Falcon 7X	Red.	No	No
Embraer 175	Red.	Yes	Yes‡
Embraer 190	Red.	Yes	Yes‡
Fokker 100	Red.	No	No

**Advanced model available for some types*

†Equipped with different engines than the sonAIR model

‡KLM Cityhopper

B. B737NG maximum levels

The $L_{A,max}$ results for the B737NG can be seen in Figure 12.

C. Boeing 777-300ER

The Boeing 777-300ER (B77W) was also considered for this research. This aircraft has the advantage that for sonAIR an advanced emission model is available, which would allow for comparison between reduced and advanced model results. Since the advanced model concerns airframe noise, this comparison can be best made for landings. The simulation results for both models and Doc29 can be seen in Figure 13.

Mean results deviate greatly and a large spread is visible for both sonAIR models, with $\Delta L_{AE}^{adv} = -2.48 \pm 5.16$ dBA and $\Delta L_{AE}^{red} = 4.08 \pm 5.27$ dBA. Doc29 results are slightly better, with $\Delta L_{AE} = -1.10 \pm 4.25$ dBA. The $L_{A,max}$ results are not shown here, but are for sonAIR $\Delta L_{AE}^{adv} = -5.21 \pm 6.09$ dBA and $\Delta L_{AE}^{red} = 0.64 \pm 5.34$ dBA, and for Doc29 $\Delta L_{AE} = -4.20 \pm 4.59$ dBA.

Looking into the cause of these large differences, it was found that the NOMOS measurements used for this analysis are of insufficient quality. Noise events have low $L_{A,max}$ and/or no clear peak in the noise level, which makes it difficult to distinguish the event from the background noise. An example noise event graph can be seen in Figure 14, which is taken from the ANOMS software [8].

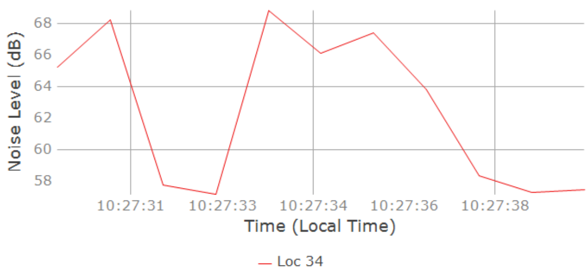

Fig. 14 Example noise event graph for B77W landing

A relevant analysis can only be carried out if more, adequate data is available. Due to the scarcity of FDR data, this was not possible at this time. However, analysing the B77W remains interesting for future research.

Acknowledgements

The author would like to thank Empa for providing the required software and emission models to perform the validation study of sonAIR. The author would also like to thank KLM for supplying the FDR data and Royal Schiphol Group for the NOMOS data.

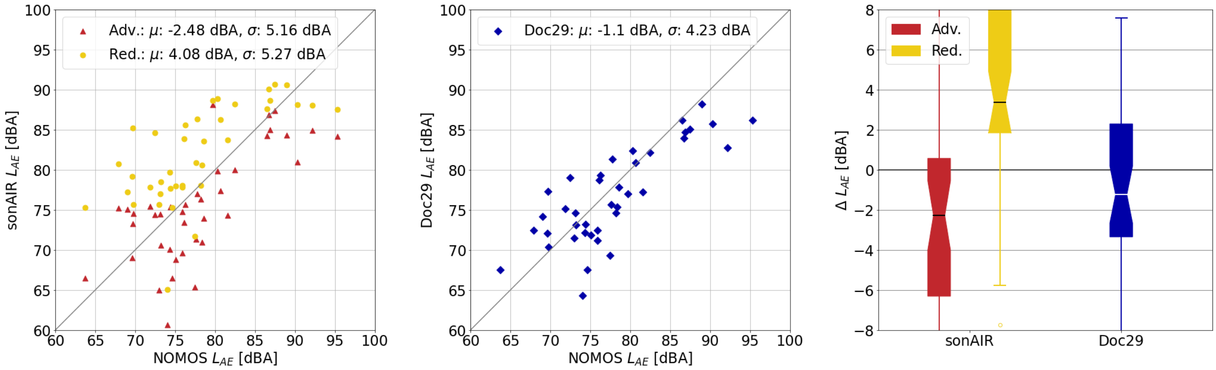

Fig. 13 Comparison of L_{AE} for B77W arrivals (39 events)

References

[1] Morrell, S., Taylor, R., and Lyle, D., "A review of health effects of aircraft noise," *Australian and New Zealand Journal of Public Health*, Vol. 21, No. 2, 1997, pp. 221–236. https://doi.org/10.1111/J.1467-842X.1997.TB01690.X.

[2] Filippone, A., "Aircraft noise prediction," *Progress in Aerospace Sciences*, Vol. 68, 2014, pp. 27–63. https://doi.org/10.1016/J.PAEROSCI.2014.02.001.

[3] Merino-Martínez, R., Heblij, S. J., Bergmans, D. H. T., Snellen, M., and Simons, D. G., "Improving Aircraft Noise Predictions Considering Fan Rotational Speed," *Journal of Aircraft*, Vol. 56, No. 1, 2019, pp. 284–294. https://doi.org/10.2514/1.C034849.

[4] Jäger, D., Zellmann, C., Schlatter, F., and Wunderli, J. M., "Validation of the sonAIR aircraft noise simulation model," *Noise Mapping*, Vol. 8, No. 1, 2021, pp. 95–107. https://doi.org/10.1515/NOISE-2021-0007.

[5] Schiphol, A., "Alderstafel Schiphol Technische beschrijving vliegtuig geluidmeetsystemen: Luistervink, Nomos, Sensornet," 2012.

[6] Casper BV, "NOMOS online (NL)," , 2022. URL https://noiselab.casper.aero/ams/#page=n_over_nomos.

[7] Van der Grift, R., "Aircraft Noise Model Improvement by Calibration of Noise-Power-Distance Values using Acoustic Measurements," Ph.D. thesis, 2022. URL https://repository.tudelft.nl/islandora/object/uuid%3A60db5565-068a-4a7c-b0e0-8d83b31c8f83.

[8] Envirosuite, "Airport Noise Monitoring Systems | ANOMS," , 2023. URL https://envirosuite.com/platforms/aviation/anoms.

[9] Zellmann, C., Schäffer, B., Wunderli, J. M., Isermann, U., and Paschereit, C. O., "Aircraft noise emission model accounting for aircraft flight parameters," *Journal of Aircraft*, Vol. 55, No. 2, 2018, pp. 682–695. https://doi.org/10.2514/1.C034275.

[10] Wunderli, J. M., Zellmann, C., Köpfli, M., Habermacher, M., Schwab, O., Schlatter, F., and Schäffer, B., "SonAIR – A GIS-integrated spectral aircraft noise simulation tool for single flight prediction and noise mapping," *Acta Acustica united with Acustica*, Vol. 104, No. 3, 2018, pp. 440–451. https://doi.org/10.3813/AAA.919180.

[11] Meister, J., Schalcher, S., Wunderli, J.-M., Jäger, D., Zellmann, C., Schäffer, B., and Sescu, A., "Comparison of the Aircraft Noise Calculation Programs sonAIR, FLULA2 and AEDT with Noise Measurements of Single Flights," *Aerospace*, Vol. 8, No. 388, 2021. https://doi.org/10.3390/aerospace8120388.

[12] Jäger, D., Zellmann, C., Wunderli, J. M., Simons, D. G., and Snellen, M., "Validation of the sonAIR Aircraft Noise Simulation Model-a Case Study for Schiphol Airport," *Inter-noise 2018: Impact of Noise Control Engineering*, 2018.

[13] European Civil Aviation Conference, "ECAC.CEAC Doc 29 4 th Edition Report on Standard Method of Computing Noise Contours around Civil Airports Volume 1: Applications Guide," Tech. rep., 2016.

[14] European Civil Aviation Conference, "ECAC.CEAC Doc 29 4 th Edition Report on Standard Method of Computing Noise Contours around Civil Airports Volume 2: Technical Guide," Tech. rep., 2016.

[15] European Civil Aviation Conference, "ECAC.CEAC Doc 29 4 th Edition Report on Standard Method of Computing Noise Contours around Civil Airports Volume 3, Part 1-Reference Cases and Verification Framework," Tech. rep., 2016.

[16] Schlüter, S., Weinzierl, S., and Becker, D.-I. S., "Bestimmung der Triebwerksleistung eines überfliegenden Flugzeuges durch Audio Feature Extraction," Tech. rep., 2015.

[17] Schlüter, S., and Becker, S., "Determination of aircraft engine speed based on acoustic measurements," Tech. rep., 2016.

[18] KNMI, "Uurgegevens van het weer in Nederland," , 2023. URL https://www.knmi.nl/nederland-nu/klimatologie/uurgegevens.

[19] Koster, R. P. F., "Using NOMOS measurements to assess improvements of ECAC Doc. 29 aircraft noise calculations," Ph.D. thesis, 2020. URL http://repository.tudelft.nl/.

[20] SAE, "Application of Pure-Tone Atmospheric Absorption Losses to One-Third Octave-Band Data," 2013. https://doi.org/10.4271/ARP5534.

[21] PDOK, "Actueel Hoogtebestand Nederland - AHN3," , 2022. URL https://app.pdok.nl/rws/ahn3/download-page/#.

[22] CBS, "Bestand Bodemgebruik 2017," , 2017. URL https://geodata.cbs.nl/files/Bodemgebruik/BBG2017/.

II

Literature study

1. Introduction

Aircraft noise can not only cause annoyance, it has also been linked to cause serious adverse health effects. With the practically constant rise in air traffic since the 1950s, this is more and more of a problem. Nowadays it is important to account for aircraft noise in e.g. the design of aircraft, new flight procedures and urban development. It is therefore important to accurately quantify and model aircraft noise.

This part of the report aims to inform the reader about current methods in aircraft noise measurements and modelling. Noise metrics are discussed in Chapter 2, followed by noise models in Chapter 3. The sonAIR noise model is further explained in Chapter 4. Last, NOMOS measurements are elaborated upon in Chapter 5.

2. Noise metrics

To be able to compare noise events, it is important to quantify them in meaningful metrics. This chapter discusses some basic concepts regarding noise metric. In section 2.1, A-weighting is discussed. Section 2.2 explains the sound exposure level (SEL). Lastly, section 2.3 describes the day-evening-night average.

2.1. A-weighting

A-weighting is applied to the SPL to account for the relative loudness that is perceived by humans. Some frequency ranges are amplified, whereas others are dampened, based on the 40 phon line. The correction is done per 1/3-octave band, and can be described as follows:

$$\Delta L_A = -145.528 + 98.262log(f) - 19.509(log(f))^2 + 0.975(log(f))^3. \tag{2.1}$$

The overall A-weighted sound pressure level can then be determined using the following equation:

$$L_A = 10 \cdot log\left[\sum_i 10^{\frac{SPL(i)+\Delta L_A(i)}{10}}\right], \tag{2.2}$$

with the summation over the frequency bands. The maximum noise level is denoted as $L_{A_{max}}$ and is an important noise metric.

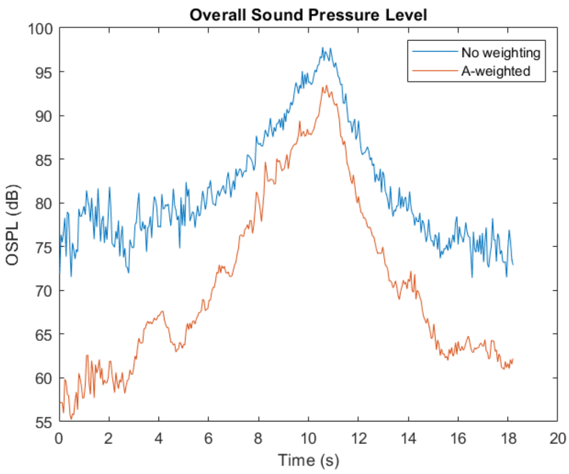

(a) Effect of A-weighting on time-series of OSPL

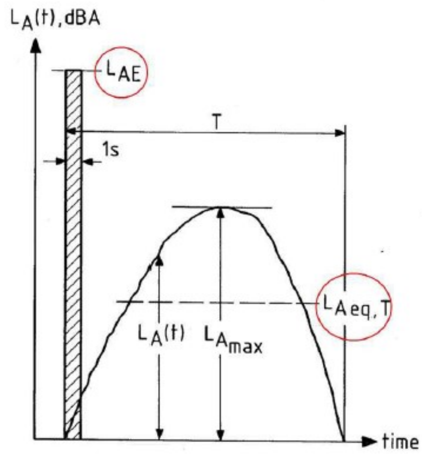

(b) Relation between SPL and SEL

Figure 2.1: A-weighting and SEL

2.2. Sound Exposure Level

The annoyance level of a sound is not only dependent on $L_{A,max}$, but also the duration of the event. To account for this influence, the Sound Exposure Level (SEL) was introduced. The SEL represents a noise event with the same energy as the original event, but squeezed within one second. It is given by:

$$L_{AE} = 10 \cdot log \left[\int_0^T 10^{\frac{L_A(t)}{10}} dt \right]. \tag{2.3}$$

The concept of SEL is visualised in Figure 2.1b.

2.3. Day-evening-night average

Another factor influencing the annoyance level is the time of day at which the noise event is taking place. A noise event at night will cause more annoyance than during the day. The day-evening-night average level (L_{DEN}) incorporates this effect, by applying weighting factors to each event. L_{DEN} is given by:

$$L_{DEN} = 10 \cdot log \left[\frac{1}{86400} \int_0^{86400} w(t) 10^{\frac{L_A(t)}{10}} dt \right], \tag{2.4}$$

where $w(t)$ is equal to 1 (0 dB) during the day (7:00-19:00), 3 (5 dB) in the evening (19:00-22:00) and 10 (10 dB) at night (22:00-7:00).

3. Noise Models

To predict and account for aircraft noise, models have been developed. In this Section an overview of the current state in aircraft noise modelling. Non-/semi-empirical models are discussed in section 3.1, followed by empirical models in section 3.2.

3.1. Non-/semi-empirical models

Non-empirical models, or theoretical models, are formed on a mathematical basis, describing the noise emission and propagation. Every aspect needs to be modelled, from the aerodynamics of the landing gear to the acoustics of the turbofan, et cetera. The advantage of such models is that a detailed noise prediction can be made for aircraft that are being developed, and thus aid in designing for minimal aircraft noise. The disadvantage however is that creating such models is a lengthy process, and the models themselves are computationally expensive. To reduce the impact of this disadvantage, measurements can be used to simplify the model, making it a semi-empirical model.

The first steps in aircraft noise prediction were taken by NASA and the FAA in the 1970s [9], when they developed the Aircraft Noise Prediction Program (ANOPP). In this model, the aircraft flight dynamics is combined with semi-empirical models for noise propagation and the emission of separate sources, such as the landing gear or flaps.

The German Aerospace Center (DLR) has also been active in the development of noise prediction models. The Parametric Aircraft Noise Analysis Module (PANAM) was mainly developed to be able to add noise as a design constraint [2] [3]. The key objective was not to achieve the highest accuracy, but rather provide a fast analysis to aid in the iterative design process. Another model developed by DLR is the SIMUL model, which models the aircraft as a sum of different noise-generating components, such as landing gear, leading edge, et cetera [2]. It uses a combination of physical modelling and measurements and is a good example of a semi-empirical model.

3.2. Empirical models

Empirical noise prediction models are based on the analysis of historical data, i.e. noise measurements. A best-practice approach is the use of Noise-Power-Distance (NPD) tables. These tables provide a noise value for an aircraft at a certain distance given its thrust setting. Advantages of this approach is that noise predictions can be made without the need for detailed information on the aircraft or its operating conditions. Due to the simplicity of the NPD tables, the models are also fast and easy to use. Disadvantages include that the models may not accurately predict noise levels for new aircraft or operating conditions that are significantly different from those in the historical data set.

An example of an empiricial noise prediction model is the Integrated Noise Model (INM) of the FAA, which was established in the late 1970s. This model considerably aided in US airport noise modelling, until it was replaced by the Aviation Environmental Design Tool (AEDT) in 2015 [5]. Similar models are used in the UK (ANCON) and Switzerland (FLULA). ANCON is used to yearly update noise contours around UK airports, in order to assist in planning policies. FLULA was developed based on flyover measurements, and is currently being replaced by sonAIR. More on sonAIR can be found in chapter 5.

In the Netherlands, an INM-based approach was also used; Nederlands Rekenmodel (NRM) has been in use since 1967. It is nowadays replaced by the European Civil Aviation Conference (ECAC) Doc.29 modelling approach. This approach is the result of the emerged need for a harmonised European approach to noise modelling. The method is described in Volume 1 [4], implementation and verification are presented in Volumes 2 and 3, respectively. The validation of Doc.29 calculations for the Schiphol airport case is discussed in Hogenhuis and Heblij [6]. In this report, Doc.29 and NRM predictions are compared to measurements around the airport (NOMOS, see chapter 4). It is concluded that, in general, Doc.29 is more accurate than NRM; however, differences remain and should be further minimised.

4. NOMOS

The NOise MOnitoring System (NOMOS) is used around Amsterdam Airport Schiphol to monitor aircraft noise. It has been active since 1993 and was developed by Brüel & Kjær.

4.1. Setup

A NOMOS station consists of a six to ten meters high tower with a calibrated microphone on top of it. This is an ISO class 1 microphone, which constantly measures all sounds in its environment [10] [1]. The measurement uncertainty of a station is 0.7 to 0.9 dB(A) [1]. The information provided by NOMOS is mainly used to inform the public, and is therefore accessible online (`nomos.schiphol.nl`). An overview of the NOMOS stations can be seen on the left side of Figure 4.1. The right side includes an example noise contour (retrieved on 27-09-2022).

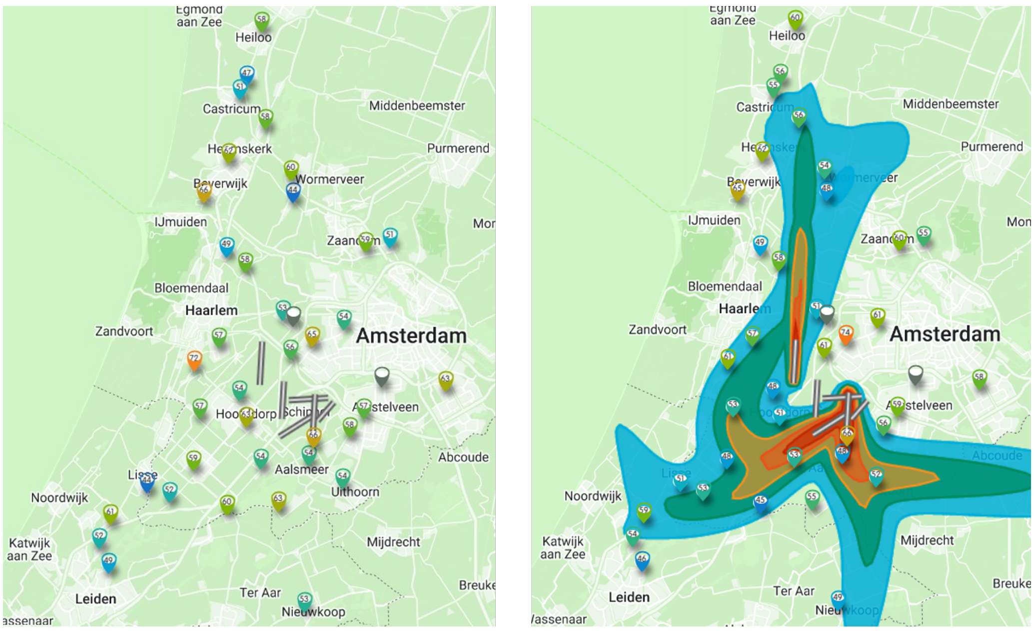

Figure 4.1: NOMOS locations and noise contour (27-09-2022) [1]

4.2. Noise Event Registration

As mentioned before, the microphone of a NOMOS station constantly measures the sound in its environment. It is thus important to be able to distinguish an aircraft-related noise event from other sounds.

Noise events are defined by fixed threshold. Each NMT has its own threshold in dB(A), depending on the background noise. The noise event starts when the measured sound passes the threshold. Further requirements on the noise events are as follows:

- The duration of the event should be at least 10 seconds and at most 120 seconds;

- The measured $L_{A_{max}}$ of the noise event must be at least $12dB(A)$ higher than the background noise level;
- This $L_{A_{max}}$ must be the local maximum for 30 seconds before and after the event;
- The SEL of the event must be between 7 and 13 dB(A) above the $L_{A_{max}}$.

5. sonAIR

The sonAIR model was created to fill the gap between best practice approaches for long-term averages (e.g. ECAC Doc.29) on one side and highly detailed, computationally expensive models (such as ...) on the other side. It is able to simulate single noise events with a high level of detail, but also perform noise mapping for airports [8]. The sonAIR model consists of two parts: an emission model and a propagation model. Each model is formulated for 24 1/3-octave bands, with mid-frequencies from 25 Hz to 5 kHz.

The emission model was established after an extensive measurement campaign at Zürich airport. This microphone data, together with FDR data, flight profiles and meteorological data, provided the input data for the backpropagation process. Based on this data, linear regression models were established for each 1/3-octave band. The emission model is further split into an airframe and engine noise model. By doing this, both sound sources can be modelled more accurately.

This method requires a lot of input data to be able to create a reliable model. This requires a lot of measurements (at different locations) for many flight events. In addition, there are obviously a lot of aircraft types, which all need their own model. As a consequence, limited aircraft types have been added to the sonAIR model. To add an aircraft type to the model, an extensive measurement campaign will have to be carried out.

5.1. Model inputs

Like any noise prediction model, sonAIR uses several input parameters. An overview of all input paramaters can be seen in Figure 5.1. The explanation of the use of each parameter is given in Zellmann et al. [12], a brief description will be presented in this section.

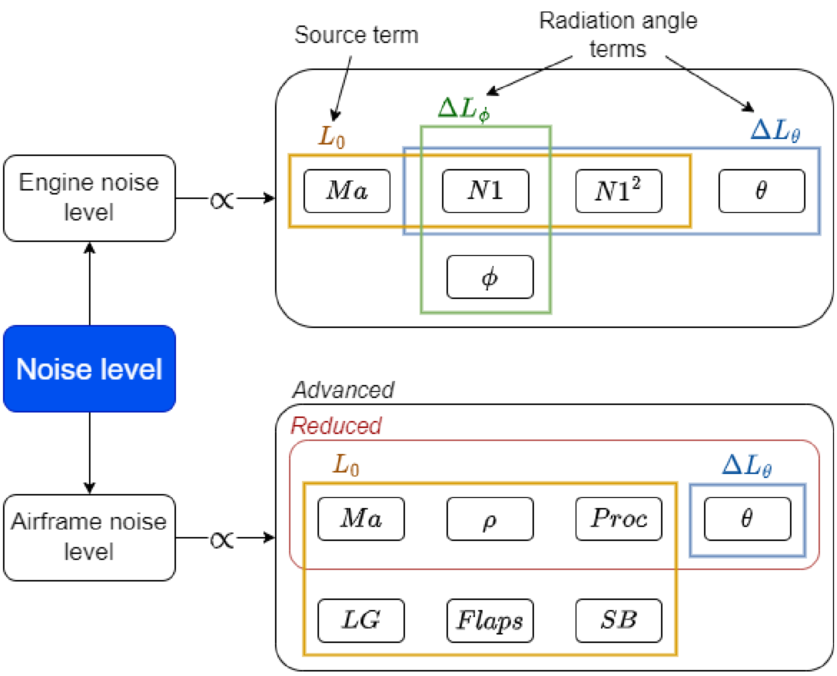

Figure 5.1: Overview of sonAIR model input parameters. (own figure)

5.1.1 N1

N1 is the engine thrust setting in %. This parameter was chosen to represent the engine, because it can be determined using spectrograms when FDR data is not available, unlike e.g. the thrust setting [11]. It is correlated to the jet velocity, which is the main cause for engine noise. To determine the relation between N1 and SPL, an engine run-up test was performed on an Airbus A330-300 with TRENT772B engine. The SPL was measured at a distance of 170 meters from the aircraft, at four locations: $15°$, $50°$, $90°$ and $120°$ respectively, with $0°$ corresponding to the nose of the aircraft. The results provided a second order polynomial for each 1/3-octave band.

5.1.2 Mach number

The aircraft Mach number is chosen to account for speed-dependent sound sources. It influences both the engine noise and airframe noise level. For engine noise, a linear relation is used. i.e. $L_{em,eng} \propto Ma$. Using the sound power level equation, a logarithmic relation is derived for airframe noise: $L_{em,afm} \propto log_{10}(Ma)$

5.1.3 Atmospheric parameters

Only the air density ρ is chosen as atmospheric parameter. The air pressure p and temperature T were omitted because of the close relation, which might lead to multicollinearity.

5.1.4 Radiation angles

The directivity of aircraft sound emission can be described using polar coordinates. The engine noise differs along the polar angle θ. There also is significant difference along the azimuth angle ϕ, which is modelled using a half-range, second order Fourier series.

5.1.5 Procedure

A binary variable is used to indicate the procedure of the aircraft. The input $Proc$ is either departure or landing. The use of this parameter will be further explained in section 5.2.

5.1.6 Airplane configuration

The airplane configuration is described in three variables: landing gear (LG, 0: retracted, 1: deployed), flap handle position ($Flaps$, 0 to 4, depending on deflection) and speed brakes (SB, 0: not deployed, 1: deployed). These inputs can only be used when FDR data is available.

5.2. Regression model

Before regression models are created, the dataset is first split in two. The first subset contains data for idle engines ($N1 \leq 40$%) and the second subset all data for engines on-load ($N1 > 40$%). The former includes only approaches, the latter both approaches and departures.

This separation of the dataset allows for the creation of two different regression models: one for airframe noise and one for engine noise.

5.2.1 Airframe model

The airframe noise model consists of a source term and a radiation term:

$$\hat{L}_{em,afm}(f) = \hat{L}_{0,afm}(lMa, l\rho, FH, LG, SB, Proc) + \Delta\hat{L}_{\theta,afm}(\theta), \tag{5.1}$$

with $lMa = log_{10}(Ma)$ and $l\rho = log_{10}(\rho/\rho_0)$. This transformation of input variables is done to ensure a linear relation with L_{em}. The variables FH, LG and SB are for the flap handle, landing gear and speedbrakes. $Proc$ stands for procedure, which is either approach or departure.

5.2.2 Engine model

The engine noise model consists of a source term and two radiation terms:

$$\hat{L}_{em,eng}(f) = \hat{L}_{0,eng}(Ma, N1, N1^2) + \Delta\hat{L}_{\theta,eng}(\theta, N1, N1^2) + \Delta\hat{L}_{\phi,eng}(\phi, N1). \tag{5.2}$$

5.2.3 Reduced model

For the case when no FDR data is available, a reduced model is available. The airplane configuration variables can no longer be used, thus the airframe model changes. The engine model remains the same.

5.3. Results

In Zellmann et al. [12], the performance of the model is evaluated using the coefficient of determination R^2 and the root mean square error $\hat{\sigma}_E$. Two aircraft are selected for a detailed evaluation, i.e. the Airbus A320 and the Embraer E170. In general, shows good correlation of the regression models with R^2_{total} between 0.7 and 0.8 approximately. The engine model performs best, with R^2_{eng} above 0.8 for almost all frequency bands. The airframe model performs less, with R^2_{afm} values between 0.2 and 0.6; however, it peaks in frequency ranges in which airframe noise is significant. The root mean square error $\hat{\sigma}_E$ shows similar behaviour for both aircraft, with values between 4.5 dB (low frequencies) to 3 dB (mid to high frequencies).

These results lead to the belief that sonAIR is a suitable model for predicting and assessing aircraft noise. The relevance of the model will increase if it will be tested and validated for more aircraft types and airports.

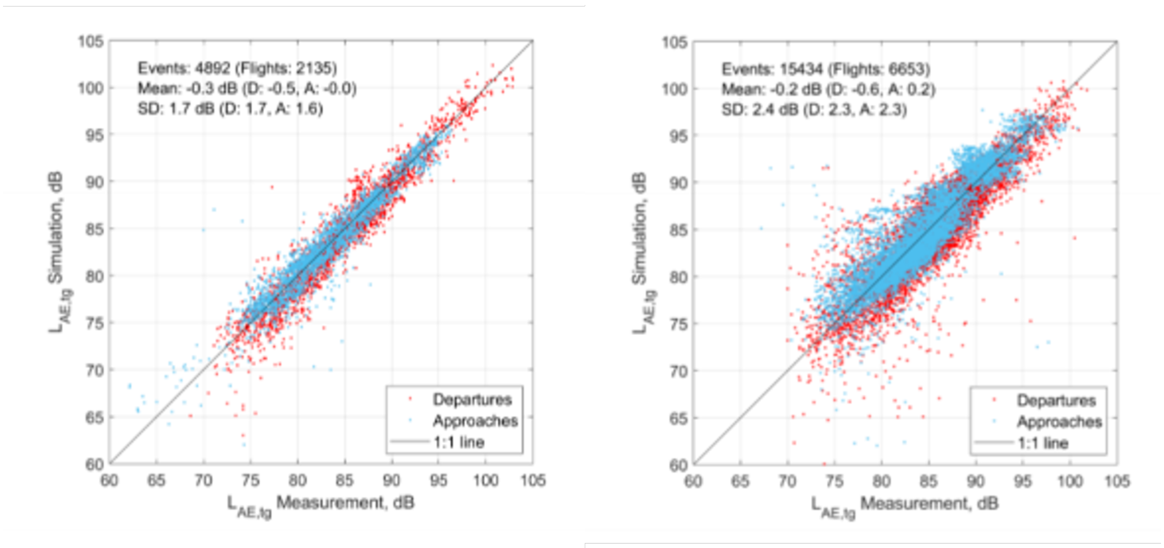

Figure 5.2: Comparison of sonAIR model results versus measurements. On the right side the reduced model, on the left side the advanced model.

5.4. Model validation

In a validation study by Jäger et al. [8], over 20,000 noise events around Zürich and Geneva airport were simulated and compared to measurements. The reduced and advanced model were evaluated separately, the results of which can be seen in Figure 5.2. Overall, the advanced models perform especially well, with almost all aircraft types having a mean difference and standard deviation below the acceptable values of $\pm$1 dB and 2 dB respectively. The reduced models show an average increase in standard deviation of about 0.7 dB. This difference may be due to the models using less information (no FDR data), both during creation and simulation.

The land cover data was identified as the most influential input parameter. Especially in urban areas, a coarse grid may not differentiate between e.g. a park and (highly reflective) buildings, which can lead to deviations.

An interesting discovery is the seasonal effect of the model accuracy. It is found that the model is quite accurate during the summer months, but underestimates the noise levels in winter. The authors suspect that this may be (partially) due to the fact that all measurements used to set up the model were conducted during spring and summer.

In another validation performed by Jäger et al. [7], sonAIR was compared to measurements around Schiphol airport in collaboration with Delft University of Technology. A total of 74 overflights were measured, using a microphone array consisting of 32 microphones on a wooden platform. The results show a mean difference of -0.4 dB, with a standard deviation of 1.1 dB. These results are a first step in showing the applicability of sonAIR to different airports, but more research is required.

III

Supporting work

6. Spectral directivity

In general, the close you are to a sound source, the louder the received noise is. However, the directivity of the sound (source) is also of interest. To analyse this effect for aircraft noise...

An example aircraft track is given in Figure 6.1, where the colour of each datapoint indicates the L_A value.

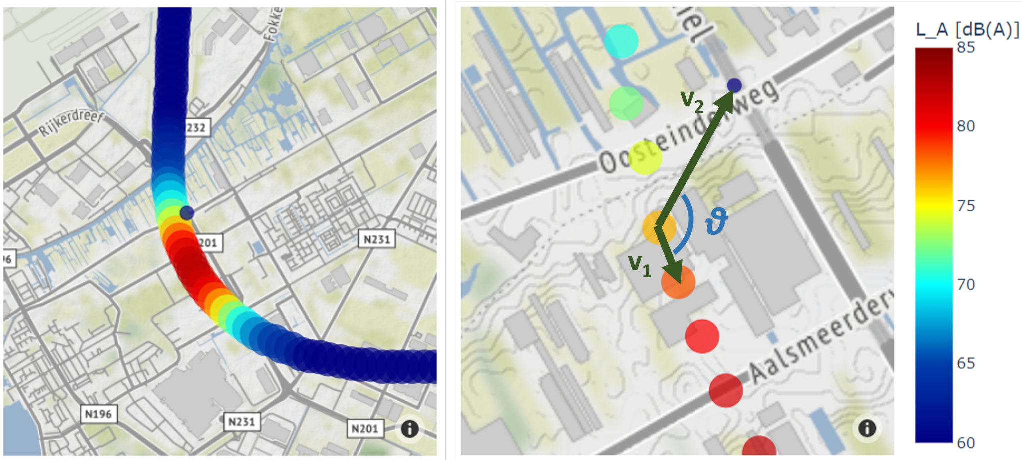

Figure 6.1: ACMS data track points of flight 02, with L_A data. The right side shows a zoomed in version with vectors v_1 and v_2.

Using the geometry as in the figure, the angle between vectors v_1 and v_2 is then given by:

$$tan(\theta) = \frac{v_1 \times v_2}{v_1 \cdot v_2}. \tag{6.1}$$

Plotting θ versus L_A gives the results as shown in Figure 6.2. To be clear, $\theta = 0°$ is in front of the aircraft and $\theta = 180°$ is behind the aircraft.

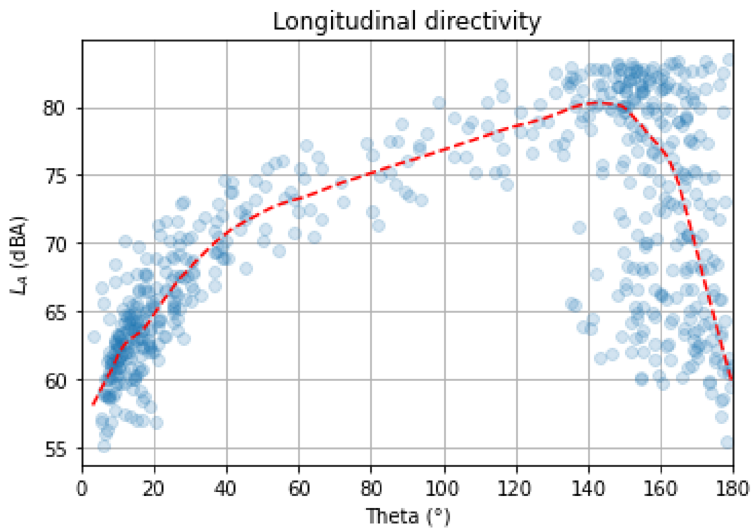

Figure 6.2: Longitudinal directivity of the B737 for departures

These values represent the modelled L_A at the NMT, corrected for propagation time. It goes without saying that the emitted sound at the source is a lot higher. It would be best to correct these values for the propagation distance. However, it was found to be difficult to do so, since no detailed sound spectrum is available at each point. Thus, the variability in distance to the source lead to some uncertainty. In addition, the azimuth angle ϕ also differs per data point.

Nevertheless, the general trend of the curve shows that the highest L_A values are behind the aircraft. This behaviour is also identified by Zellmann et al. [12], see Figure 6.3.

The curve on the left is similar to Figure 6.2. The curve on the right shows that the influence of the azimuth angle φ is limited.

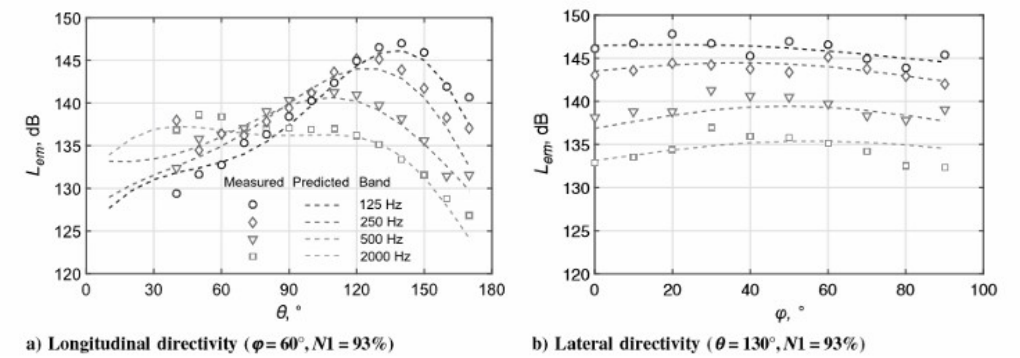

Figure 6.3: Spectral directivity of the A320 for departure at high-power setting [12]

7. Noise contour

Besides calculating noise values for NMTs, or 'Beurteilungspunkte' in German, sonAIR can also calculate values for a grid of receivers ('Empfangspunktgitter'). As a case study, one flight has been selected at random to demonstrate the applicability.

A grid of 80 by 80 points was set up, with a distance of 50 meters in between. The receiver grid and results can be seen in Figure 7.1.

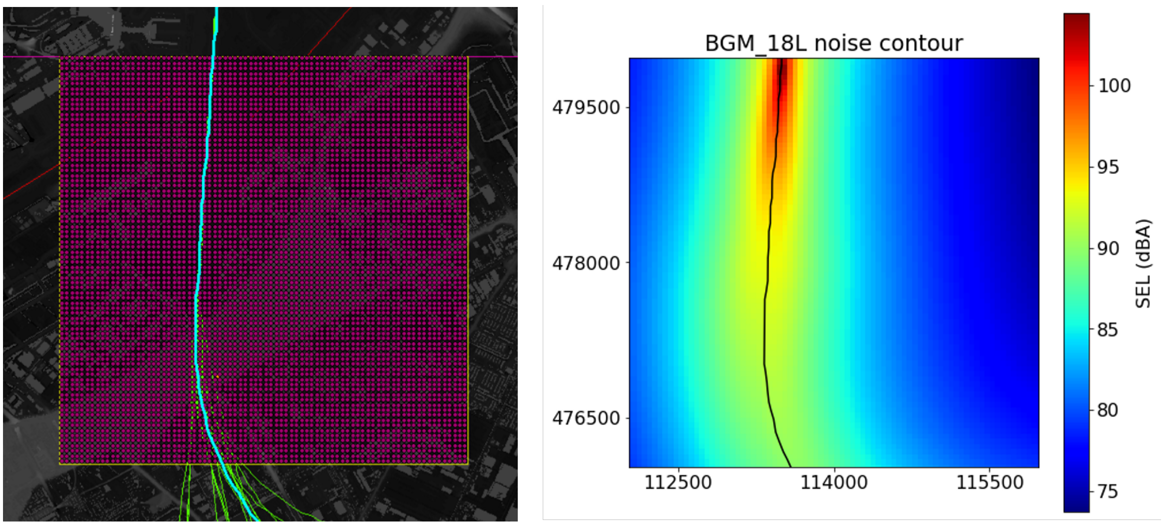

Figure 7.1: Noise contour as calculated by sonAIR. On the left side, a screenshot of ArcMap can be seen, where each purple dot represents a (virtual) receiver. The right side shows the corresponding noise contour.

It can be seen that the noise contour nicely follows the flight track.

Bibliography

[1] NOMOS online (NL). URL https://noiselab.casper.aero/ams/#page=n_over_nomos.

[2] L. Bertsch and U. Isermann. Noise prediction toolbox used by the DLR aircraft noise working group. 2013. URL https://www.researchgate.net/publication/257773363.

[3] L. Bertsch, W. Dobrzynski, and S. Guérin. Tool Development for Low-Noise Aircraft Design. *https://doi.org/10.2514/1.43188*, 47(2):694–699, 5 2012. ISSN 15333868. doi: 10.2514/1.43188. URL https://arc.aiaa.org/doi/10.2514/1.43188.

[4] European Civil Aviation Conference. ECAC.CEAC Doc 29 4 th Edition Report on Standard Method of Computing Noise Contours around Civil Airports Volume 1: Applications Guide. 2016.

[5] S. Fidell and V. Mestre. *A Guide To U.S. Aircraft Noise Regulatory Policy*. 2020. ISBN 9783030399078. doi: 10.1007/978-3-030-39908-5. URL https://doi.org/10.1007/978-3-030-39908-5.

[6] R. Hogenhuis and S. Heblij. Trendvalidatie van Doc.29 berekeningen. 2018. URL www.nlr.nl.

[7] D. Jäger, C. Zellmann, J. M. Wunderli, D. G. Simons, and M. Snellen. Validation of the sonAIR Aircraft Noise Simulation Model-a Case Study for Schiphol Airport. Technical report, 2018.

[8] D. Jäger, C. Zellmann, F. Schlatter, and J. M. Wunderli. Validation of the sonAIR aircraft noise simulation model. *Noise Mapping*, 8(1):95–107, 1 2021. ISSN 2084879X. doi: 10.1515/NOISE-2021-0007/MACHINEREADABLECITATION/RIS. URL https://www.degruyter.com/document/doi/10.1515/noise-2021-0007/html.

[9] J. P. Raney. Development of a new computer system for aircraft noise prediction. 3 1975. doi: 10.2514/6.1975-536. URL http://arc.aiaa.org.

[10] A. Schiphol. Alderstafel Schiphol Technische beschrijving vliegtuig geluidmeetsystemen: Luistervink, Nomos, Sensornet.

[11] J. M. Wunderli, C. Zellmann, M. Köpfli, M. Habermacher, O. Schwab, F. Schlatter, and B. Schäffer. SonAIR – A GIS-integrated spectral aircraft noise simulation tool for single flight prediction and noise mapping. *Acta Acustica united with Acustica*, 104(3):440–451, 5 2018. ISSN 18619959. doi: 10.3813/AAA.919180.

[12] C. Zellmann, B. Schäffer, J. M. Wunderli, U. Isermann, and C. O. Paschereit. Aircraft noise emission model accounting for aircraft flight parameters. *Journal of Aircraft*, 55(2):682–695, 9 2018. ISSN 15333868. doi: 10.2514/1.C034275/ASSET/IMAGES/LARGE/FIGURE17.JPEG. URL https://arc.aiaa.org/doi/10.2514/1.C034275.